View metadata, citation and similar papers at core.ac.uk
brought to you by CORE
provided by UCL Discovery

SUPPORTING INFORMATION

Scalable high-affinity stabilization of magnetic iron oxide nanostructures by a biocompatible antifouling homopolymer

Giovanni Luongo[1], Paola Campagnolo[1,2], Jose E. Perez[3], Jürgen Kosel[3], Theoni K. Georgiou[1], Anna Regoutz[1], David J. Payne[1], Molly M. Stevens[1,4], Mary P. Ryan[1], Alexandra E. Porter[1], and Iain E. Dunlop[1]*

[1] Department of Materials, Imperial College London, London SW7 2AZ, United Kingdom.

[2] School of Biosciences and Medicine, Faculty of Health and Medical Sciences, University of Surrey, Guildford, GU2 7XH.

[2] King Abdullah University of Science and Technology, Thuwal 23955, Kingdom of Saudi Arabia.

[4] Department of Bioengineering and Institute for Biomedical Engineering, Imperial College London, London SW7 2AZ, United Kingdom.

* Corresponding Author i.dunlop@imperial.ac.uk

KEYWORDS: magnetic nanoparticles, biocompatible nanoparticles, surface functionalization, iron oxide, magnetite, maghemite, poly(MPC), surface-adsorbed polymers.

Additional Materials and Methods

Materials

Synthesis of poly(MPC) homopolymer and random copolymer

2-Methacryloyloxyethyl phosphorylcholine, poly(ethylene glycol) methyl ether 2-bromoisobutyrate (MPC), 2,2′-Bipyridyl (bpy, ReagentPlus® ≥99%), copper(I) bromide (purum p.a. 98.0% (RT)), tetrahydrofuran (THF, anhydrous ≥99.9% inhibitor-free), azide-fluor 545 (Carboxytetramethylrhodamine-azide) and ethanol anhydrous denatured were purchased from Sigma-Aldrich; Propargyl methacrylate (PMA, 98% stabilised with 250ppm 4-methoxyphenol) was purchased from VWR. For dialysis, Biotech regenerated cellulose (RC) membrane 3.5-5kD was purchased from Spectrum Labs. For ^{1}H-NMR, Methanol-d4 (MeOD, 99.8 atom % D) was purchased from Sigma-Aldrich. Water is (18.2 MΩ·cm, Milli-Q® direct water purification system) throughout.

Detailed Methods for Polymer Characterization

^{1}H-NMR

The polymer samples were investigated with an AV400 NMR Bruker spectrometer running with TopSpin software. The samples were dissolved to a concentration of 10mg/ml in deuterated methanol (MeOD). One dimensional ^{1}H NMR spectra were obtained at 400Hz by acquiring 16 scans over the sample. All NMR spectra were acquired at room temperature. The data were processed with MestReNova software and OriginPro 9.1 to identify the proton chemical shifts. The data were reported relative to the MeOD solvent (MeOD, δ 4.870 ppm).

Gel permeation chromatography (GPC)

The molecular weight distribution of the polymeric samples was investigated by Agilient 1260 Infinity Multi-Detector GPC instrument at a flow rate of 0.7 mL/min through PL aquagel–OH

column (PL aquagel-OH MIXED-M 8 μm, Agilient) at 40 °C. The samples were dissolved to a final concentration of about 3mg/ml in an aqueous solution of 0.03M sodium nitrate ($NaNO_3$) and 0.01M monosodium phosphate (NaH_2PO_4) with 2% ethanol (EtOH) added as a flow rate marker. Heavy metal chelating beads (Cuprisorb, Fish Fish Fish, UK) were added to the solution for 5h to remove copper contaminations and it was subsequently filtered with a 0.22 μm PTFE filter. The instrument is provided with both refractive index (RI) and UV detectors. The RI signal was used to determine the M_w relative to PEO standards (Agilient Technologies, UK) without corrections. The UV detector was set to a wavelength of 545nm to allow the detection of the fluorescent moieties "clicked" to the samples.

Fourier Transform Infrared Spectroscopy (FTIR)

FTIR spectra were acquired with Perkin Elmer Spectrum 100 in Attenuated Total Reflection (ATR) mode. The spectra were processed with OriginPro 9.1 to identify the relevant bands through the use of standard tables[8].

Transmission electron microscopy (TEM)

TEM imaging

All TEM modes (bright-field TEM, high-angle aperture dark field scanning TEM (HAADF-STEM) and STEM-energy dispersive X-ray spectroscopy (STEM-EDX) were performed with a JEOL JEM-2100F instrument operated at an accelerating voltage of 200 kV. For cryo-TEM imaging only, low dose-imaging acquisition conditions were used to reduce specimen damage during focusing and images were acquired at a dose lower than 10 $e^-/Å^2$. Where required, brightness and contrast were adjusted using ImageJ.

Staining of grid-deposited samples with uranyl acetate

The staining protocol was adapted from the literature[1]. 2% uranyl acetate (UA) was dissolved in ultrapure water and stored for 24h at 4 ˚C. Drops of this staining solution (5 µl) were released on each TEM grid containing the samples to stain. During the staining the grids are held at 45° to allow the excess solution to flow away and six drops of UA are released. The grids were then blotted with filter paper, leaving a thin film which was allowed to air-dry.

Sample preparation for cryo-TEM

A Leica EM GP instrument was used for rapid plunge freezing of thin films of sample solution into liquid ethane. A drop of 5 µl of solution containing the sample was deposited on TEM grids, which had been mounted onto the instrument. The samples were stored in liquid nitrogen and transferred to the JEOL JEM-2100F TEM operated in BF-TEM mode at 200 kV. Low dose-imaging acquisition conditiom,s were used to reduce specimen damage during focusing and images were acquired at a dose lower than 10 $e^-/Å^2$. The same protocol as for the BF-TEM samples was adopted to operate a tiling sampling to confirm the stability of the solution without any user bias.

X-ray Photoelectron Spectroscopy (XPS)

XPS measurements

XPS spectra were acquired with a Thermo Scientific K-Alpha+ X-ray Photoelectron Spectrometer (XPS) system operating at $2x10^{-9}$ mbar base pressure. This system incorporates a monochromated, microfocused Al Kα X-ray source (hν = 1486.6 eV) and a 180° double focusing hemispherical analyser with a 2D detector. The X-ray source was operated at a 6 mA emission current and 12 kV anode bias. Data were collected at 200 eV pass energy for survey and 20 eV pass energy for core level and valence band spectra using an X-ray spot size of 400 μm^2. A flood gun was used to minimize sample charging. Spectra were aligned assuming the C

1s core line to be at a binding energy of 285.0 eV. All data were analysed using the Avantage software package.

Sample preparation for XPS

For the nanowire oxidation state measurements (Fig S.5A,B), magnetite-maghemite nanowire samples in ultrapure water were collected with a magnetic separator (MidiMACS™ Separator), resuspended in ethanol and ultrasonicated for 10 min. The procedure was repeated for a total of 5 times and the volume of ethanol was kept at 50 μl after the final wash. A 10 μl drop was deposited on a silicon substrate and dried in air. The magnetic separator (MidiMACS™ Separator) was placed below the substrate to favour a high concentration of sample in a reduced area. In measurements for the validation of the rinsing protocol, the polycarbonate membrane was removed after electrodeposition by successive rinses with DCM as described in the main text. Aliquots for XPS measurements were removed at 1, 2, 10 rinsing steps, and measured as for the nanowire oxidation state measurements.

X-ray Diffraction (XRD)

XRD of iron oxide nanowires embedded in their polycarbonate template were acquired with (X'Pert^3 Powder, PANalytical, 2θ measured in the range 10°- 75°). The samples were bound to the holder with adhesive.

Dynamic light scattering (DLS)

DLS measurements used the Malvern Zetasizer Nano range instrument to measure the stability of the functionalised nanoparticles. Samples of non-functionalised and functionalised nanoparticles (0.05 mg/ml in water) were prepared as for bright-field TEM above, and analysed after 10min sonication. The dispersion state for each sample was monitored for approximately 9h/sample. Z-averages were calculated using the instrument software.

Scanning Electron Microscopy

Images were acquired using FEG-SEM (LEO Gemini 1525, measured at 5 keV; JEOL JSM 6010LA, measured at 20 keV). Samples were deposited on Si substrates that had been cleaned with piranha solution (30% hydrogen peroxide solution and sulphuric acid mixed in 1:3 ratio, 2 hours incubation; Safety Warning! Piranha solution is highly oxidizing and evolves heat – use only with detailed risk assessment) rinsed with ultrapure water and dried with a nitrogen flow. Cross-sectional samples were cut and mounted on an SEM pin holder (Agar Scientific).

Reflectance mode bright-field optical microscopy

Bright field reflectance mode optical images of functionalised and non-functionalised nanowires were acquired with a UPLFLN-P strain-free 20x objective mounted on Olympus BX51-P microscope operated with Olympus Stream software. The nanowire solution (≈ 10 µl) was deposited on clean glass slides and coverslips were applied. The samples were imaged directly after preparation in order to show the aggregation state of the nanowires according to a previously established protocol[2].

Cytotoxicity assays

Cell seeding: The cells were grown in complete medium to confluence and then thoroughly rinsed with PBS and PBS-EDTA before adding Trypsin (5 ml) and incubating them for 2 minutes at 37 °C. The enzyme activity was blocked by adding an equivalent amount of medium. The cells were counted using a haemocytometer, a total of 16×10^6 cells were washed by centrifugation (300 rpm for 5 min) and resuspended in cell medium to a total volume of 80 ml. A total of 20,000 cells were plated in each well of 96 well plates and incubated at 37 °C. Each plate contained 4 technical replicates for each time point incubation with the nanowires and an untreated control for normalization.

Treatment with nanowires: Similar amounts of non-coated iron/iron oxide core-shell nanowires (≈1 × 10^9, KAUST) and poly(MPC) coated (refer to protocol above) nanowires were washed with phosphate buffered saline (PBS). The coated and non-coated nanowires were collected by magnetic separation (Magna-Sep™ , Invitrogen), resuspended in PBS (1 ml) and ultrasonicated (10 mins). The washing process was repeated 5 times, with the final step reduced to a volume of 200 μl, which was then aliquoted to deliver to 250 and 500 nanowires/cell respectively and added to the cells in complete medium.

Cell viability measurements: Viability was determined at the indicated time points by Alamar Blue assay (ThermoFisher), following the manufacturer protocol. Cells were incubated with 100 μl per well of AlamarBlue reagent diluted 1:10 in cell medium. After 2h incubation, the redox level of the AlamarBlue was quantified on a plate reader by reading the fluorescence of each well (excitation 544 nm, emission 590 nm) and expressed as a percentage of the control reading from each plate (i.e. the identical cells incubated without nanowires).

Gel permeation chromatography (GPC) of poly(MPC) and poly (MPC-*co*-PMA)

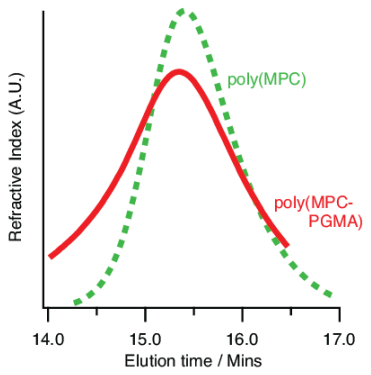

Polymer	Mn / kDa	Dispersity = Mn / Mw
poly(MPC)	8500	1.18
Poly(MPC-co-PMA)	11500	1.26

Figure S.1. GPC elution curves for poly(MPC) and poly(MPC-co-PMA); corresponding molecular weights and dispersities determined by calibration with PEG standards.

UV-vis spectroscopy of poly(MPC-*co*-PMA) reacted with azide-Fluor

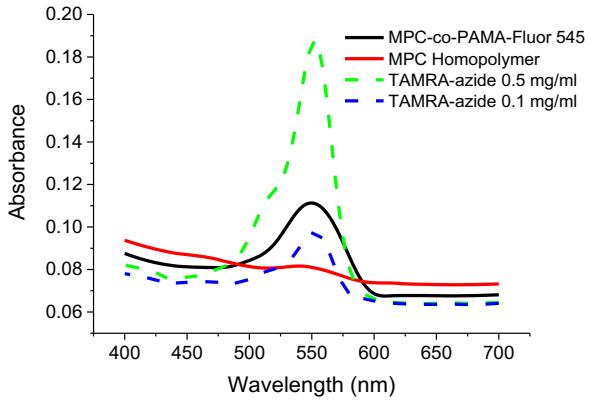

Figure S.2 UV-vis spectrum around 545 nm of poly(MPC-*co*-PMA) reacted with azide-Fluor545 (solid black line), a control sample of MPC homopolymer incubated with azide-Fluor545 [TAMRA-azide] under identical conditions (solid red line) and calibration solutions of azide-Fluor545 at 0.1 mg/ml (dashed blue line) and 0.5 mg/ml (dashed green line).

Characterization of electrodeposited magnetite-maghemite nanowires

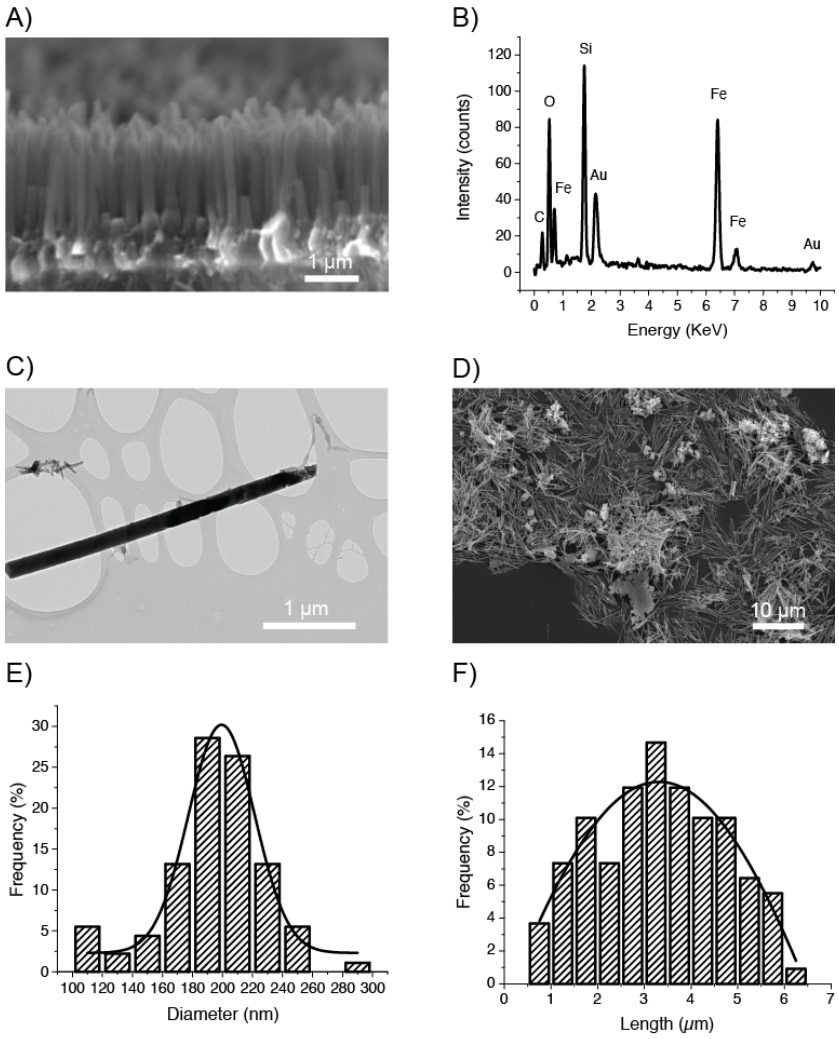

Figure S.3. Morphology and composition of magnetite-maghemite nanowires. A) Side view of nanowires on copper substrate (SEM after dissolution of polycarbonate membrane and sputtering of thin gold film. B) Energy-dispersive X-ray spectroscopy (EDX) shows iron as the dominant component of the nanowires. C) Close-up of individual nanowire after release from template and copper film (TEM). D) Nanowire population after release (SEM, allowed to dry on silicon substrate). The histograms represent the length distribution E) and diameter distribution F) of the nanowires, giving an average length of 3.31 ± 0.12 μm and diameter of 199 ± 2 nm.

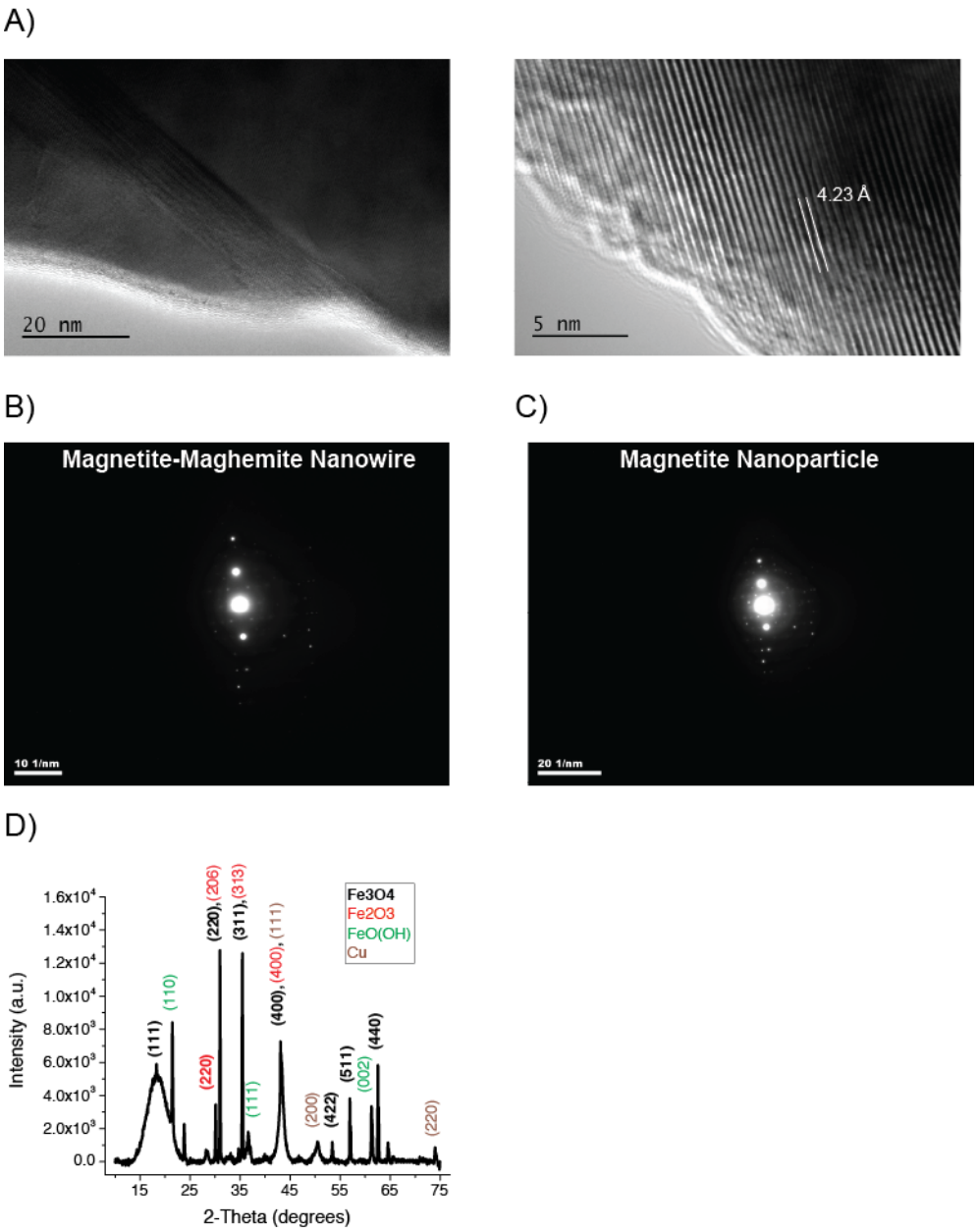

Figure S.4. Structural analysis of magnetite-maghemite nanowires. A) High resolution TEM images showing the interface between different crystals (left) and the lattice fringes at 4.23 ± 0.31 Å (centre) corresponding to the (123) spacing of γ-Fe_2O_3[25] B) C) Small angle X-ray diffraction pattern of magnetite-maghemite nanowire closely resembles that of commercial magnetite nanoparticle. D) Indexed X-ray diffraction pattern showing peaks consistent with a mixture of magnetite and maghemite, with possible traces of Goethite.

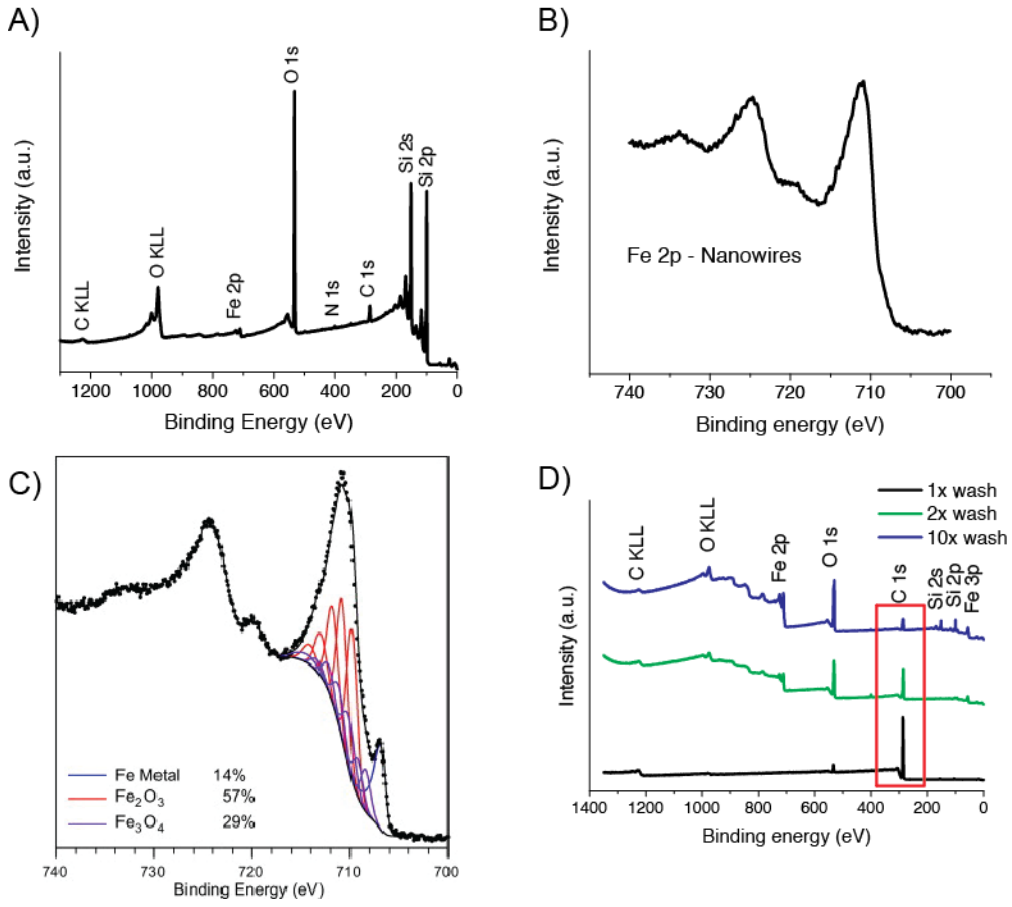

Figure S.5. A) Broad scan XPS spectrum of magnetite-maghemite nanowires, showing elemental composition; B) High resolution structure of the Fe 2p binding energy, compared with C) the Fe 2p spectrum of a mixed iron oxide[3]. The spectrum suggests the presence of both Fe_3O_4 and γ-Fe_2O_3 in the nanowires sample (see text). D) XPS-based optimization of the rinsing protocol following nanowire extraction from polycarbonate electrodeposition template. Substantial residual polycarbonate remains after 1 rinsing step in DCM, as shown by a high C 1s signal and poor visibility of the Fe 2p peak. The situation is rectified after 10 rinsing steps. Image C is reproduced with permission from Reference 3. Copyright 2010 Elsevier.

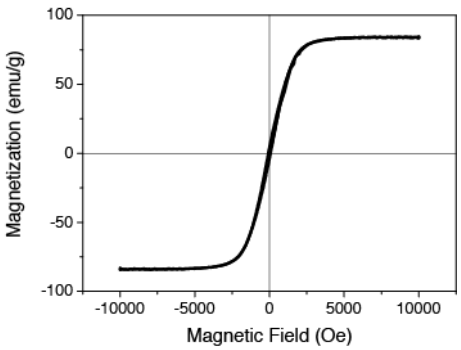

Figure S.6. Vibrating sample magnetometry of iron oxide nanowires in polycarbonate membrane showing a soft material with a magnetic moment in between that of bulk magnetite and maghemite.

References

(1) Hajibagheri, M. Electron Microscopy: Methods and Protocols. *Methods Mol. Biol. N. Y., N.Y., U. S.* **1999**, *117*.

(2) Theodorou, I. G.; Botelho, D.; Schwander, S.; Zhang, J.; Chung, K. F.; Tetley, T. D.; Shaffer, M. S. P.; Gow, A.; Ryan, M. P.; Porter, A. E. Static and Dynamic Microscopy of the Chemical Stability and Aggregation State of Silver Nanowires in Components of Murine Pulmonary Surfactant. *Environ. Sci. Technol.* **2015**, *49* (13), 8048–8056.

(3) Biesinger, M. C.; Payne, B. P.; Grosvenor, A. P.; Lau, L.; Gerson, A. R.; Smart, R. S. C. Resolving Surface Chemical States in XPS Analysis of First Row Transition Metals, Oxides and Hydroxides: Cr, Mn, Fe, Co and Ni. *Appl. Surf. Sci.* **2011**, *257* (7), 2717–2730.